Title: A critical role for MSI1 and MSI2 in photoreceptor morphogenesis

Authors: Jesse Sundar[1], Fatimah Matalkah[1], Bohye Jeong[1], Peter Stoilov[1]*, and Visvanathan Ramamurthy[1,2,3,]*

Affiliations: Departments of Biochemistry[1], Ophthalmology and Visual Sciences[2], and Neuroscience[3]; Robert C. Byrd Health Sciences Center, West Virginia University; Morgantown, West Virginia, USA, 26505;

Address for correspondence:

Peter Stoilov, Department of Biochemistry, West Virginia University School of Medicine; 1 Medical Center Dr. Morgantown, WV, USA, 26505; Email: pstoilov@hsc.wvu.edu; Telephone: 304-293-6334; Fax: 304-293-6846;

Visvanathan Ramamurthy, Department of Biochemistry, West Virginia University School of Medicine; 1 Medical Center Dr. Morgantown, WV, USA, 26505; Email: ramamurthyv@hsc.wvu.edu; Telephone: 304-293-2479; Fax: 304-293-6846;

Keywords: Msi1, Msi2, Musashi, Retina, Photoreceptor, RNA-binding protein, Splicing.

ABSTRACT

We previously proposed a role for the Musashi proteins, MSI1 and MSI2, in photoreceptor cell development that is mediated by their ability to control alternative splicing. Photoreceptors with simultaneous deletion of Msi1 and Msi2 did not respond to light, displayed severely disrupted OS morphology and axonemal defects. At postnatal day 5, we observed an increase in proliferating retinal progenitor cells in the knockout animals, suggesting delay in photoreceptor development. The loss of Musashi prevented the use of photoreceptor-specific exons in transcripts important for OS morphogenesis, ciliogenesis and synaptic transmission. However, deletion of the photoreceptor-specific exons in Ttc8, Cc2d2a, Cep290, Cacna2d4, and Slc17a7 did not impair retinal development or visual function. We demonstrate a critical role for Musashi in the morphogenesis of terminally differentiated photoreceptor neurons. This role is in stark contrast with the canonical function of the two proteins in maintenance and renewal of stem cells.

INTRODUCTION

In eukaryotes, alternative splicing of pre-mRNA is a process that increases protein diversity and controls gene expression. Diversification of proteomes through alternative splicing is a defining characteristic of metazoans and was expanded dramatically in bilaterians[1]. Alternative splicing is particularly prevalent in vertebrate neurons and is critical for the development and function of vertebrate nervous systems[2–7].

We previously showed that photoreceptor neurons exploit a unique splicing program[8]. Motif enrichment analysis suggested that Musashi-1 (MSI1) and Musashi-2 (MSI2), promote the use of photoreceptor specific exons[8]. We further showed that MSI1 is critical for utilization of photoreceptor specific exon in Tetratricopeptide repeat domain protein-8 (Ttc8)[8]. In addition, Musashi promotes the splicing of several photoreceptor specific exons when over-expressed in cultured cells[8]. Recently, analysis of a comprehensive gene expression data set that spanned multiple tissues and cell types from mice and human proved that photoreceptors utilize a unique set of alternative exons that are primarily regulated by MSI1 and MSI2[9]. Furthermore, the work by Ling et. al. demonstrated that Msi1 transcript levels are upregulated in the developing rod photoreceptors and reach exceptionally high levels compared to all other cell types or tissues in the data set.

The MSI1 and MSI2 proteins have two highly conserved RNA binding domains (RBDs) in the N-terminal region which show close to 90% sequence identity and recognize a similar UAG motif in RNA[10]. The two RBDs of MSI1 and MSI2 are followed by a less conserved C-terminal region which shows approximately 70% sequence identity[11]. The high degree of sequence identity between the MSI1 and MSI2 results in functional redundancy between the two proteins[12,13]. The canonical function of the Musashi proteins is to control mRNA translation in

the cytosol[14,15], where they can either block or enhance translation of mRNA depending on cellular context[16–21].

Vertebrate photoreceptors are neurons specialized in detecting and transducing light stimuli. Photoreceptors are characterized by segmented morphology which compartmentalizes phototransduction, core cellular functions, and synaptic transmission. The light sensing machinery is confined to the outer segment, a stack of membranes that is elaborated by cell's modified primary cilium. The outer segment is dynamic structure that is remade every 7 to 10 days. Consequently, maintenance of the outer segment requires high rate of transport of membranes and proteins through the connecting cilium[22].

Interestingly, the predicted splicing targets of Musashi in photoreceptors include pre-mRNAs from ciliary (Ttc8, Cep290, Cc2d2a, Prom1) and synaptic-associated genes (Cacna2d4, Slc17a7)[23–29]. These genes have been showed to be crucial for photoreceptor development and fucntion[23–29]. We proposed that production of photoreceptor specific splicing isoforms that is promoted by Musashi is necessary for the development and maintenance of photoreceptor cells *in vivo*[8].

To test if Musashi drives photoreceptor development and function, we removed *Msi1* and *Msi2* in the developing retina and rod photoreceptor cells. We find that Musashi proteins are essential for photoreceptor function, morphogenesis, and survival but not their specification. Specifically, the Musashi proteins are crucial for outer segment (OS) and axoneme development. As expected, disruption of the Musashi genes led to loss of expression of photoreceptor specific splicing isoforms. Surprisingly, deleting the photoreceptor-specific exons of the, *Ttc8*, *Cc2d2a*, *Cep290*, *Cacna2d4*, and *Slc17a7* genes does not produce a detectable phenotype suggesting that the loss of vision in the Musashi mutants is likely independent of the role of the Musashi proteins

85 in controlling alternative splicing.

86

87

MATERIALS AND METHODS

Generation of mice and genotyping

Mice carrying floxed alleles for *Msi1* and *Msi2* were provided by Dr. Christopher Lengner from the University of Pennsylvania. *Six3-Cre* transgene or *Nrl-Cre* transgenes were used to delete the floxed alleles in developing retina or rod photoreceptors. All mouse lines were devoid of naturally occurring *rd1* and *rd8* alleles[30,31]. Males hemizygous for the *Six3-Cre* transgene or *Nrl-Cre* transgene and floxed for either *Msi1*, *Msi2*, or both *Msi1* and *Msi2* were mated with females floxed for either *Msi1*, *Msi2*, or both *Msi1* and *Msi2* to obtain experimental knockout mice and littermate control. The offspring of breeding pairs were genotyped using PCR of DNA derived from ear biopsies. The *Msi1* wildtype and floxed alleles were identified using following primers: (5'-CGG ACT GGG AGA GGT TTC TT-3' and 5'-AGC TCC CCT GAT TCC TGG T-3')[32]. The *Msi2* wildtype and floxed alleles were identified by using following primers: (5'-GCT CGG CTG ACA AAG AAA GT-3' and 5'-TCT CCT TGT TGC GCT CAG TA-3')[32]. The presence of the *Six3 Cre* transgene was determined using following primers: (5'-CCC AAA TGT TGC TGG ATA GT-3' and 5'-CCC TCT CCT CTC CCT CCT-3'). The presence of the *Nrl Cre* transgene was determined using following primers: (5'-TTT CAC TGG CTT CTG AGT CC-3' and 5'-CTT CAG GTT CTG CGG GAA AC-3'). The presence of *Cre* recombinase was determined using following primers: (5'-CCT GGA AAA TGC TTC TGT CCG-3' and 5'-CAG GGT GTT ATA AGC AAT CCC-3')[33].

The knockout of the photoreceptor specific exons in Ttc8, Cep 290, and Cc2d2a was done using CRISPR/Cas9. Two guide RNAs were used for each alternative exon to target intronic sites upstream and downstream of the alternative exons to cause their deletion. The guide RNAs were commercially synthesized by Synthego and had the following targeting

sequences: Ttc8-1 GUUCCUGGAAAGCGUUAAGA, Ttc8-2 CAGCACAUUUUCCAAUCUUC, Cep290-1 CCCUAAGGGUAGUUAAAGCU, Cep290-2 CGUUUGUUCUUCAAAAGGAC, Cc2d2a-1 GCAUGUCACUCAUCUACCAU, and Cc2d2a-2 AGCGUUUAACUGAUGACUGC. The guide RNAs and Cas9 (Thermo Fisher) were assembled into RNPs and electroporated into zygotes by the WVU transgenics core facility. The founders were back-crossed to wild type C57 Black 6/J for 5 generations to eliminate off-target mutations. The deleted exons were genotyped using the following primers: Ttc8-CRISP-F ctccccatcctagccaatct, Ttc8-CRISP-R tgtgcacaggcaaaataagc, Cep290-CRISP-F gagcaaacacagcagtcagc, Cep290-CRISP-R tcttctgaccgccacctact, Cc2d2a-CRISP-F gctacacacatggctggatg, Cc2d2a-CRISP-R ctctcatgtgacaggcagga.

All experiments were conducted with the approval of the Institutional Animal Care and Use Committee at West Virginia University. All experiments were carried out with adherence to the principles set forth in the ARVO Statement for the Ethical Use of Animals in Ophthalmic and Vision Research which advocates the use of the minimum number of animals per study needed to obtain statistical significance.

Electroretinography, Immunoblotting, and Reverse Transcriptase PCR

Electroretinography, immunoblotting, and reverse transcriptase PCR were conducted using previously described protocol from our laboratory[8,34,35].

Immunofluorescence Microscopy

Immunofluorescence microscopy was carried out using a modified procedure in our laboratory[34,35]. Briefly, eyes were enucleated, and the cornea and lens were discarded. After dissection, eyes were fixed by immersion in 4% paraformaldehyde in PBS for one hour. After washing the eyes in PBS three times for ten minutes each, they were dehydrated by overnight

incubation in 30% sucrose in PBS. Eyes were then incubated in a 1:1 solution of OCT:30% sucrose in PBS for one hour and frozen in OCT (VWR). The frozen tissues were sectioned using a Leica CM1850 cryostat for collecting serial retinal sections of 16μm thickness. The retinal cross-sections were then mounted onto Superfrost Plus microscope slides (Fisher Scientific). Slide sections were then washed and permeabilized with PBS supplemented with 0.1% Triton X-100 (PBST) and incubated for one hour in a blocking buffer containing 10% goat serum, 0.3% Triton X-100, and 0.02% sodium azide in PBS. Retinal sections were then incubated with primary antibody in a dilution buffer containing 5% goat serum, 0.3% Triton X-100, 0.02% sodium azide, and primary antibody at 1:500 dilution in PBS overnight at 4ºC followed by three 5 minute washes using PBST. Sections were then incubated in the same dilution buffer containing secondary antibody and DAPI at 1:1000 for one hour. Slides were washed with PBST three times for five minutes each before treating with Prolong Gold Antifade reagent (ThermoFisher) and securing the coverslip. The images were collected using a Nikon C2 Confocal Microscope.

Retinal histology of the mouse models

Following euthanasia, eyes were enucleated using a C-shaped forceps after marking the superior pole and incubated in Z-fixative for >48 hours before shipment and tissue processing by Excalibur Pathology Inc. (Norman, OK)[34,35]. The embedding, serial sectioning, mounting, and hematoxylin/eosin (H&E) staining were performed by Excalibur Pathology. A Nikon C2 Microscope equipped with Elements software was used to image the slides.

Transmission Electron Microscopy

After euthanasia, a C-shaped forceps was used to enucleate the eye, and the cornea was discarded[34,35]. Eyes were then incubated in a fixative solution containing 2.5% glutaraldehyde

and 2% paraformaldehyde in 100mM sodium cacodylate buffer at pH 7.5 for 45 minutes before removal of the lens. After lensectomy, eyes were placed back into fixative for 72 hours before shipment, tissue processing, and imaging at the Robert P. Apkarian Integrated Electron Microscopy Core at Emory University.

Antibodies

The following primary antibodies were used throughout our studies: rat anti-MSI1 (1:1000; Medical and Biological Laboratories, Woburn, MA), rabbit anti-MSI2 (1:2000; Abcam, Cambridge, MA), mouse anti-β-tubulin (1:10,000; Sigma-Aldrich, St. Louis, MO), rabbit anti-phospho-histone H3 (1:500; Cell Signaling, Danvers, MA), mouse anti-Ki67 (1:500; BD Biosciences, San Jose, CA), rabbit anti-active Caspase-3 (1:500; Promega, Madison, WI), rhodamine peanut agglutinin (1:1000; PNA: cone OS sheath marker, Vector laboratories, Burlingame, CA), rabbit anti-peripherin-2 (1:2000) was a kind gift by Dr. Andrew Goldberg from Oakland University, rabbit anti-PDE6β (1:2000; ThermoFisher, Waltham, MA), mouse anti-acetylated α-tubulin (1:1000; Santa Cruz, Dallas, TX), guinea pig anti-MAK (1:500; Wako, Richmond, VA), mouse anti-glutamylated tubulin (1:500; AdipoGen Life Sciences, San Diego, CA), mouse anti-Ttc8 (1:1000; Santa Cruz, Dallas, TX), rabbit anti-Ttc8 Exon 2A (1:1000; custom made[8]), mouse anti-GAPDH (1:10,000; Fitzgerald, Acton, MA), and 4′,6-diamidino-2-phenylindole (DAPI: nuclear counterstain; 1:1000; ThermoFisher, Waltham, MA).

RESULTS

Validation of the conditional knockout mouse models

We analyzed the expression of Musashi proteins in various tissues from adult mice. Out of all the tissues we tested, retina showed the highest expression of MSI1 and MSI2 proteins (Figure 1A), in line with the previously reported high transcript levels for *Msi1* and *Msi2* in rod photrecptors[9]. To test the biological significance of Musashi protein expression in the murine retina, we used *Cre-LoxP* conditional recombination to remove either *Msi1*, *Msi2*, or both the *Msi1* and *Msi2* genes throughout the entire retina and ventral forebrain using the *Six3 Cre* transgene (Supplementary Figure 1)[36]. Throughout this work, we refer to *Musashi* floxed mice which are hemizygous for the *Six3 Cre* transgene as *ret-Msi-/-* mice. The conditional recombination results in the deletion of *Msi1's* transcription start site, exon 1, and exon 2 (Supplementary Figure 1)[13]. For *Msi2*, the transcription start site and the first four exons are removed after cre-mediated recombination (Supplementary Figure 1)[13]. The ablation of MSI1 and MSI2 was confirmed by immunoblotting retinal lysates from knockout mice at postnatal day 10 (PN10) (Figure 1B). Immunofluorescence microscopy of retinal cross sections obtained from the knockout mice also affirmed the absence of MSI1 and MSI2 expression in the retina (Figure 1C). Notably, MSI2 protein levels were moderately but reproducibly upregulated in *Msi1* knockout retina (Figure 1B, Supplementary Figure 2). We did not observe the inverse, upregulation of MSI1 protein in *Msi2* knockouts (Supplementary Figure 2). These data show that MSI1 protein regulates the expression of MSI2 and could indicate existence of a homeostatic mechanism for regulation overall Musashi protein levels.

The Musashi proteins are crucial for photoreceptor function

To determine if the Musashi proteins are required for photoreceptor function, we

performed electroretinographic (ERG) recordings of the *Musashi* conditional knockout mice at PN16 and monitored for changes in retinal function up to PN180. Figure 2A shows the scotopic and photopic ERG waveforms of the *ret-Msi1-/-*, *ret-Msi2-/-*, and *ret-Msi1-/-:Msi2-/-* mice at PN16 immediately after mice open their eyes[37]. When both *Musashi* genes are removed, no scotopic or photopic retinal function remains as shown by absence of conspicuous "a"-waves and "b"-waves (Figure 2A). However, significant retinal function remains in the *ret-Msi1-/-* and *ret-Msi2-/-* single knockout mice. We characterized the retinal function of the *ret-Msi1-/-* and *ret-Msi2-/-* mice further to see if there was a photoresponse deficit at higher light intensities or as the mice aged (Figure 2B-E). In *ret-Msi1-/-* mice, there was a statistically significant reduction in photoreceptor "a"-wave amplitudes at almost all light intensities (Figure 2B). This reduction in the photoreceptor "a"-wave amplitude persisted in *ret-Msi1-/-* mice up to PN180 (Figure 2C). On the other hand, *ret-Msi2-/-* mice at PN16 had normal photoreceptor function at all the light intensities we tested (Figure 2D). The "a"-wave amplitude began to decrease progressively in *ret-Msi2-/-* mice as they aged, and this became significant at PN120 (Figure 2E). Overall, this data shows that the Musashi proteins essential for photoreceptor function, and the two proteins are partially redundant.

Intrinsic expression of Musashi in photoreceptors is crucial for photoreceptor function

We next sought to determine if the phenotype of the *ret-Msi-/-* mice was due to the absence of Musashi protein expression in photoreceptors or if deletion of Musashi in other retinal cell types or retinal progenitors were contributing to the loss of vision. To this end, we generated rod-specific *Musashi* conditional knockouts by crossing *Musashi* floxed mice with mice hemizygous for the *Nrl Cre* transgene where the *Nrl* promoter activates Cre expression in rod photoreceptors[38]. Throughout this work, we refer to the *Musashi* floxed mice that are

hemizygous for the *Nrl Cre* transgene as *rod-Msi-/-* mice. After confirming the loss of Musashi proteins in rod photoreceptors (Supplementary Figure 3), we used ERG to analyze the retinal function of the knockout mice after ablation of the *Musashi* genes in rods (Supplementary Figure 4A-E). Supplementary Figure 4A shows the scotopic and photopic ERG waveforms of the *rod-Msi1-/-*, *rod-Msi2-/-*, and *rod-Msi1-/-:Msi2-/-* mice at PN16. As observed in the *ret-Msi1-/-:Msi2-/-* mice, no conspicuous rod function was observed in the *rod-Msi1-/-:Msi2-/-* mice at PN16 which is demonstrated by absence of conspicuous "a"-wave under scotopic testing conditions (Supplementary Figure 4A). Again, we examined the *rod-Msi1-/-* and *rod-Msi2-/-* single knockout mice further to see if the photoresponse phenotype was comparable to that obtained from the *ret-Msi1-/-* and *ret-Msi2-/-* mice. In *rod-Msi1-/-* mice at PN16, there was a reduction in photoreceptor "a"-wave amplitudes at multiple light intensities (Supplementary Figure 4B). This reduction in "a"-wave amplitude persisted as these mice aged up to PN180 (Supplementary Figure 4C). Contrarily, PN16 *rod-Msi2-/-* mice had no changes in photoreceptor function at all the light intensities examined (Supplementary Figure 4D). As observed in the *ret-Msi2-/-* mice, the "a"-wave amplitude began to decrease progressively as these mice aged, and this decrease became statistically significant at PN90 (Supplementary Figure 4E). The similar phenotypes of the *ret-Msi* and *rod-Msi* knockout mice shows that the intrinsic expression of Musashi proteins in photoreceptors is crucial for their function and that deletion of Musashi proteins in other cell types likely does not contribute significantly to the phenotype observed in the *ret-Msi-/-* mice. Therefore, throughout the rest of our studies, we focus on the *ret-Msi1-/-:Msi2-/-* mouse model for our experiments since there is a compensation in function occurring between MSI1 and MSI2 in the single knockout mice and to avoid confounding results that might be obtained when *Msi1* and *Msi2* are deleted only in rod but not cone photoreceptors.

246 **Retinal cell death occurs in the absence of the Musashi proteins**

247 We next wanted to examine the mechanism behind the photoreceptor dysfunction seen in
248 the *ret-Msi1-/-:Msi2-/-* mouse model. One of the common causes of a reduced ERG is
249 photoreceptor cell death. Therefore, we performed histological analysis of the *ret-Msi1-/-:Msi2-*
250 */-* mice at PN5, PN10, PN16, and PN180 (Figure 3A-D). In *ret-Msi1-/-:Msi2-/-* mice at PN5,
251 even before the neural retina has differentiated completely, there is a reduction in the neuroblast
252 layer (NBL) thickness which was quantified across the superior-inferior axis (Figure 3A, left and
253 right panels). There is also a more disordered arrangement of NBL nuclei in *ret-Msi1-/-:Msi2-/-*
254 mice with cells more tightly packed together compared to its littermate control (Figure 3A, left
255 panel). At PN10, the outer nuclear layer (ONL), inner nuclear layer (INL), and ganglion cell
256 layer (GCL) of the retina all form in *ret-Msi1-/-:Msi2-/-* mice but there is a reduction in the
257 number of layers of photoreceptor nuclei (Figure 3B, left and right panels). At PN16, the number
258 of layers of ONL nuclei continue to decrease suggesting that photoreceptor cell death is
259 occurring (Figure 3C, left and middle panels). However, at this age, there are no statistically
260 significant changes in the number of layers of INL nuclei (Figure 3C, left and right panels). By 6
261 months of age, the retina of *ret-Msi1-/- :Msi2-/-* mice was severely degenerated with a complete
262 loss of ONL nuclei in addition to a significant reduction in the number of layers of INL nuclei
263 (Figure 3D, left, middle, and right panels).

264 **Changes in proliferation during retinal development in the absence of MSI1 and MSI2**

265 After observing a significant reduction in NBL nuclei in *ret-Msi1-/-:Msi2-/-* mice even
266 before their retinas had fully differentiated, we wanted to investigate if this phenotype is related
267 to the proliferation or premature death of retinal progenitor cells (RPCs). We collected retinal
268 cross sections of *ret-Msi1-/-:Msi2-/-* mice at PN5 and probed with antibodies against phospho-

histone H3 (PHH3) and Ki67, which are two commonly used markers of proliferation[39–41]. We also examined apoptosis of retinal cells in *ret-Msi1-/-:Msi2-/-* mice by staining with an antibody against the apoptotic marker anti-active Caspase-3 (CASP3)[40,42]. In *ret-Msi1-/-:Msi2-/-* mice, we witnessed a substantial increase of both PHH3+ and Ki67+ cells within the central retina whereas the littermate control had very few PHH3+ and Ki67+ cells within the central retina (Figure 4A and B). We also noticed a trend toward increase of PHH3+ and Ki67+ cell in the peripheral retina of *ret-Msi1-/-:Msi2-/-* mice (Figure 4A and B). No significant changes in proliferation marker staining were witnessed when comparing the superior and inferior retina of *ret-Msi1-/-:Msi2-/-* mice. CASP3 staining of retinal cross sections from *ret-Msi1-/-:Msi2-/-* mice showed no significant differences in the number of CASP3+ cells in either the central or peripheral retina (Figure 4C). Our data points to altered proliferation and not increased apoptosis at early stages of retinal development as the cause for the reduced number of NBL nuclei at PN5 in the Musashi knockout mice.

The Musashi proteins are required for OS development

Photoreceptor cells are present in the *ret-Msi1-/-:Msi2-/-* as indicated by the well-defined ONL (Figure 3C). We therefore examined the structure of the OS in *ret-Msi1-/-:Msi2-/-* mice at PN16 by immunofluorescence microscopy using three different OS markers, anti-Peripherin-2 (PRPH2: OS marker), anti-Phosphodiesterase-6β (PDE6β: rod OS marker), and peanut agglutinin (PNA: cone OS marker). After staining retinal cross sections from *ret-Msi1-/-:Msi2-/-* mice with PRPH2 and PNA, we observed a severe shortening of the photoreceptor outer segment (Figure 5A). This result was not limited to PRPH2, as staining with the rod OS marker PDE6β demonstrated the same phenotype (Figure 5B). The outer segment of cone photoreceptors also appears to be severely shortened as shown by the abnormal PNA staining (Figure 5A-B). This

defect is likely independent of degeneration since a similar change was observed at PN10 before significant degeneration (Supplementary Figure 6). Lastly, no mislocalization of PDE6β or PRPH2 is found in the ONL or inner segment of *ret-Msi1-/-:Msi2-/-* mice suggesting that while the Musashi proteins are required for outer segment formation they are not regulating trafficking or localization of OS-resident proteins (Figure 5B).

The Musashi proteins are crucial for photoreceptor outer segment and axoneme development

Using transmission electron microscopy, we imaged ultrathin retinal sections from *ret-Msi1-/-:Msi2-/-* mice at PN10 when the OS begins to elaborate (Figure 6). When examining the OS/IS boundary in *ret-Msi1-/-:Msi2-/-* mice by electron microscopy, we observed very little, if any, conspicuous OS (Figure 6A). Instead, the IS of the *ret-Msi1-/-:Msi2-/-* mice appears to come in direct contact with the RPE (Figure 6A-B). At higher magnification, the photoreceptors of *ret-Msi1-/-:Msi2-/-* mice displayed either no OS or aberrant and undersized OS (Figure 6B left, middle, and right panels). The basal body and connecting cilium (CC) appear to be normal in structure and size (Figure 6B, middle panel).

To further examine the structure of the connecting cilium and the axoneme, we stained retinal cross sections from *ret-Msi1-/-:Msi2-/-* mice at PN10 using antibodies directed against the connecting cilium (glutamylated and acetylated α-tubulin) and axoneme (MAK) markers[40,43–45]. Probing with glutamylated and acetylated α-tubulin antibodies showed that there were no changes in the length of the CC (Figure 7A, C-D). Contrarily, staining with the anti-MAK antibody showed a substantial reduction in the length of the axoneme accompanied with punctate staining suggesting a severe structural defect of the axoneme (Figure 7A-B).

The Musashi proteins promote splicing of photoreceptor specific exons

Our previous studies suggested that the Musashi proteins are regulating alternative splicing of their target pre-mRNAs in vertebrate photoreceptors[8]. To test if the Musashi proteins are responsible for the inclusion of photoreceptor specific exon , we analyzed the splicing in *ret-Msi1-/-:Msi2-/-* mice of pre-mRNAs from cilia-and OS-related genes that we previously showed to express photoreceptor specific isoforms (Figure 8). We witnessed a drastic reduction in alternative exon inclusion in *ret-Msi1-/-:Msi2-/-* mice for all tested transcripts (Figure 8B). We analyzed isoform expression at the protein level for Ttc8 using two different antibodies, a pan-antibody that recognizes all Ttc8 protein isoforms (Pan-Ttc8) and the other that recognizes the photoreceptor-specific isoform of Ttc8 by binding the epitope encoded by Exon 2A (the photoreceptor-specific exon of *Ttc8*) (Figure 8A, bottom panel). After probing retinal lysates from the *ret-Msi1-/-:Msi2-/-* mice with the pan-Ttc8 antibody, we observed faster migration of the Ttc8 protein compared to the littermate control suggesting that the Exon 2A was not included (Figure 8C). Concordantly, when probing for the photoreceptor-specific isoform of Ttc8 using the Ttc8 Exon 2A antibody, we saw an absence of this isoform in *ret-Msi1-/-:Msi2-/-* mice (Figure 8C). Taken together, these results demonstrate that the Musashi proteins are required for the inclusion of photoreceptor specific alternative exons.

Alternative exons included in photoreceptor mRNAs are not required for photoreceptor cell development

To examine the biological significance of the photoreceptor-specific splicing program that is regulated by the Musashi proteins, we used CRISPR-Cas9 to delete the photoreceptor-specific exons from the *Ttc8, Cc2d2a, Cep290, Cacna2d4,* and *Slc17a7* genes in *C57BL6/J* mice. These exons were chosen because: (i) they are in genes critical for vision; (ii) the exons are used specifically in photoreceptors where nearly all of the transcripts include the exon; (iii) the exons

with exception of the Slc17a7 exon are conserved in vertebrates. After validating the exon knockout mice (Figure 9A), we collected ERG traces from the exon knockout mice to determine if these exons were necessary for the function of rod and cone photoreceptor cells. Figure 9B shows ERG traces from the *Ttc8* exon knockout, *Cep290* exon knockout, *Cc2d2a* exon knockout, *Cacna2d4* exon knockout, and *Slc17a7* exon knockout compared to wildtype (far left). No significant changes in retinal function were observed in any of exon knockout mice compared to control by five months of age (Figure 9B) suggesting that the inclusion of these photoreceptor-specific exon inclusion is not critical for rod and cone function.

DISCUSSION

MSI1 and MSI2 are required for photoreceptor morphogenesis but not specification

Our data shows the requirement for MSI1 and MSI2 in photoreceptor cells. Double knockout of *Msi1* and *Msi2* in retinal progenitors results in complete loss of vision. Two lines of evidence demonstrate that this loss of vision is due to a defect in photoreceptor morphogenesis, rather than developmental defects due to impairment of the retinal progenitor cells. First, the specification of retinal progenitors to photoreceptor cells was not affected by loss of Musashi. The retina of the knockout mice had clearly defined outer nuclear layer. The rod photoreceptor nuclei retained their characteristic morphology, and the photoreceptor cells expressed cell type specific transcripts such as peripherin and PDE6β. Importantly, knockout of *Msi1* and *Msi2* in rod photoreceptors driven by *Nrl-Cre* caused loss of scotopic photoresponse. Thus, the vision phenotype is not due to impairment of the early stages of retinal development and is caused by a defect specific to photoreceptor cells.

Morphological examination by electron microscopy and immunofluorescence showed that the outer segment of the photoreceptors lacking Musashi is either missing or is stunted and disorganized. The absence of outer segment is accompanied by a shortened axoneme. In contrast, the connecting cilium has normal length and did not have obvious defects. Trafficking of PDE6 and peripherin through the connecting cilium also appears to be normal and the two proteins localize to the stunted outer segment wherever one is present. Taken together our findings demonstrates a requirement for Musashi in the morphogenesis and function of the photoreceptor outer segment that appears not to affect transport along the connecting cilium.

Normal photoreceptor function in photoreceptor-specific exon knockout mice

RT-PCR analysis of alternative splicing in the retina of *Msi1* and *Msi2* knockout mice showed that inclusion of photoreceptor specific exons in the mature transcripts is dependent on the Musashi proteins. Even though MSI1 and MSI2 regulate the splicing of the Ttc8, Cc2d2a, Cep290, Cacna2d4, and Slc17a7 pre-mRNAs, knockouts of the photoreceptor specific-exons in these genes revealed that these exons are not crucial for photoreceptor function. The retina of the exon knockout animals developed normally, and no adverse phenotype was observed up to 5 months after birth. Thus, our data does not support a mechanism by which alternative splicing mediates the phenotype of the Musashi knockouts in photoreceptor cells. This is a surprising result considering that four out of the exons are conserved and the genes that host them are critical for vision. Based on the currently available data we cannot completely rule out role for splicing in shaping the phenotype of the Musashi knockouts. Nevertheless, our results point that other mechanism need to be explored, particularly in the light of the documented role for Musashi in control mRNA translation.

Cell proliferation and survival in the Musashi knockout retina

Morphological examination showed reduced cell number in the neuroblastoid layer at postnatal day 5 in the knockout animals. In the mature retina the outer nuclear layer did not reach the size of the corresponding layers in the wild type animals and progressively degenerated with age. The MSI1 protein was previously reported to be required for photoreceptor survival, but no loss of inner neurons was reported, likely due to the presence of the paralogous MSI2[46]. The reduction of the inner nuclear layer that we observe demonstrate that the Musashi proteins are required for the survival of inner retinal neurons in addition to photoreceptors. Interestingly, the reduction of the neuroblastic layer in the Musashi knockout retina at postnatal day 5 was accompanied by increase in the number of proliferating cells that stained positive for PHH3 and

Ki67. Caspase 3 staining did not show differences in the number of apoptotic cells between the wild type and the knockout retina at that stage. These apparently contradictory observations can be explained with the role of the Musashi proteins in supporting stem cell renewal and proliferation through activation of the Notch pathway[16,47–50]. We propose that loss of Musashi in the developing retina reduces the numbers and proliferation rates of the neuronal precursors leading to delayed development of the neuroblastoid layer.

Functional redundancy within the Musashi protein family

In vertebrates, the Musashi protein family consists of two paralogues, MSI1 and MSI2, which have high degree of sequence identity, and have arisen from a gene duplication event[51,52]. The RNA binding domains of MSI1 and MSI2 have approximately 90% sequence identity and recognize the same UAG sequence motif *in vitro* and *in vivo*[53–56]. The high degree of similarity suggest that the two proteins are likely to be functionally redundant when co-expressed in the same cells. Indeed, we observed only minor reductions in visual function after the loss of either MSI1 or MSI2 alone whereas the combined loss of MSI1 and MSI2 resulted in a complete loss of visual function (Figure 2). Similarly, inclusion of photoreceptor specific exons is promoted by both proteins, and the double knockout produces stronger effect on splicing than the knockouts of either *Msi1* or *Msi2*. The functional redundancy in photoreceptor cells that we observe is in agreement with previous reports of redundancy between MSI1 and MSI2 in other cell types[12,13].

The redundancy between the two Musashi proteins in the retina appear to be partial. Loss of MSI1 produce more severe phenotype than loss of MSI2. Specifically, we observe an early visual defect in the *Msi1* knockout mice, which is absent in the *Msi2* knockouts. Loss of MSI1

also produced a stronger effect on splicing compared to MSI2. This partial redundancy may reflect intrinsic functional differences between the two proteins, or simply difference in their expression levels in photoreceptor cells. Interestingly, we noticed moderate but reproducible increased in the MSI2 protein levels after knocking out *Msi1* (Supplementary Figure 2). Such mutual regulation can contribute to the redundancy between the two proteins and be a part of a homeostatic mechanism that maintains the overall Musashi protein levels.

Our work highlights roles for MSI1 and MSI2 in retinal development, retinal cell survival and photoreceptor morphogenesis. An interesting aspect of the function of the Musashi proteins in retina our their apparently mutually exclusive roles at different stages of development. At early stages of development MSI1 and MSI2 support the renewal and proliferation of retinal precursor cells. At late stages of retinal development and in the adult retina MSI1 and MSI2 are required for morphogenesis of the differentiated photoreceptor cells and survival of mature neurons. These roles are likely executed through translational control of Musashi targets, as knockouts of alternative exons regulated by the Musashi proteins did not recapitulate any of the aspects of the phenotype of the Musashi knockout mice. Future studies will be aimed at determining the mechanism(s) by which the absence of Musashi causes a complete loss of vision in mice.

FUNDING

This work was supported by the National Institutes of Health [grant numbers RO1 EY028035, R01 EY025536, and R21 EY027707]; the West Virginia Lions Club Foundation; and International Lions Club Foundation.

ACKNOWLEDGEMENTS

The authors thank Maxim Sokolov, John Hollander, Ronald Gross for their feedback on the work. We also thank Dr. Christopher Lengner for the generous donation of the *Msi1fl/fl Msi2fl/fl* mice and Dr. Andrew Goldberg for PRPH2 antibody.

AUTHOR CONTRIBUTIONS

P.S. and V.R. jointly conceived and supervised this study, and edited the manuscript. J.S. designed and performed experiments, and wrote the manuscript. F.M. and B.J. designed and performed experiments.

CONFLICTS OF INTEREST

The authors declare no conflicts of interest.

REFERENCES

1. Grau-Bové, X., Ruiz-Trillo, I. & Irimia, M. Origin of exon skipping-rich transcriptomes in animals driven by evolution of gene architecture. *Genome Biol.* **19**, 135 (2018).
2. Li, Y. I., Sanchez-Pulido, L., Haerty, W. & Ponting, C. P. RBFOX and PTBP1 proteins regulate the alternative splicing of micro-exons in human brain transcripts. *Genome Res.* gr.181990.114 (2014) doi:10.1101/gr.181990.114.
3. Irimia, M. *et al.* A Highly Conserved Program of Neuronal Microexons Is Misregulated in Autistic Brains. *Cell* **159**, 1511–1523 (2014).
4. Jensen, K. B. *et al.* Nova-1 Regulates Neuron-Specific Alternative Splicing and Is Essential for Neuronal Viability. *Neuron* **25**, 359–371 (2000).
5. Gehman, L. T. *et al.* The splicing regulator Rbfox1 (A2BP1) controls neuronal excitation in the mammalian brain. *Nat Genet* **43**, 706–711 (2011).
6. Ule, J. *et al.* Nova regulates brain-specific splicing to shape the synapse. *Nat. Genet.* **37**, 844–852 (2005).
7. Vuong, C. K. *et al.* Rbfox1 Regulates Synaptic Transmission Through the Inhibitory Neuron Specific vSNARE Vamp1. *Neuron* **98**, 127-141.e7 (2018).
8. Murphy, D., Cieply, B., Carstens, R., Ramamurthy, V. & Stoilov, P. The Musashi 1 Controls the Splicing of Photoreceptor-Specific Exons in the Vertebrate Retina. *PLOS Genet.* **12**, e1006256 (2016).
9. Ling, J. P. *et al.* ASCOT identifies key regulators of neuronal subtype-specific splicing. *Nat. Commun.* **11**, 1–12 (2020).
10. Ohyama, T. *et al.* Structure of Musashi1 in a complex with target RNA: the role of aromatic stacking interactions. *Nucleic Acids Res.* **40**, 3218–3231 (2012).

478 11. Sakakibara, S., Nakamura, Y., Satoh, H. & Okano, H. RNA-Binding Protein Musashi2:
479 Developmentally Regulated Expression in Neural Precursor Cells and Subpopulations of Neurons in
480 Mammalian CNS. *J. Neurosci.* **21**, 8091–8107 (2001).
481 12. Sakakibara, S. *et al.* RNA-binding protein Musashi family: Roles for CNS stem cells and a
482 subpopulation of ependymal cells revealed by targeted disruption and antisense ablation. *Proc. Natl.*
483 *Acad. Sci.* **99**, 15194–15199 (2002).
484 13. Li, N. *et al.* The Msi Family of RNA-Binding Proteins Function Redundantly as Intestinal
485 Oncoproteins. *Cell Rep.* **13**, 2440–2455 (2015).
486 14. Kudinov, A. E., Karanicolas, J., Golemis, E. A. & Boumber, Y. Musashi RNA-Binding Proteins as
487 Cancer Drivers and Novel Therapeutic Targets. *Clin. Cancer Res.* **23**, 2143–2153 (2017).
488 15. Fox, R. G., Park, F. D., Koechlein, C. S., Kritzik, M. & Reya, T. Musashi Signaling in Stem Cells and
489 Cancer. *Annu. Rev. Cell Dev. Biol.* **31**, 249–267 (2015).
490 16. Imai, T. *et al.* The Neural RNA-Binding Protein Musashi1 Translationally Regulates Mammalian
491 numb Gene Expression by Interacting with Its mRNA. *Mol. Cell. Biol.* **21**, 3888–3900 (2001).
492 17. Battelli, C., Nikopoulos, G. N., Mitchell, J. G. & Verdi, J. M. The RNA-binding protein Musashi-1
493 regulates neural development through the translational repression of p21WAF-1. *Mol. Cell. Neurosci.*
494 **31**, 85–96 (2006).
495 18. Ma, X. *et al.* Msi2 Maintains Quiescent State of Hair Follicle Stem Cells by Directly Repressing the
496 Hh Signaling Pathway. *J. Invest. Dermatol.* **137**, 1015–1024 (2017).
497 19. Cragle, C. & MacNicol, A. M. Musashi Protein-directed Translational Activation of Target mRNAs
498 Is Mediated by the Poly(A) Polymerase, Germ Line Development Defective-2. *J. Biol. Chem.* **289**,
499 14239–14251 (2014).
500 20. Rutledge, C. E. *et al.* Efficient Translation of Dnmt1 Requires Cytoplasmic Polyadenylation and
501 Musashi Binding Elements. *PLOS ONE* **9**, e88385 (2014).

21. MacNicol, M. C. *et al.* Evasion of regulatory phosphorylation by an alternatively spliced isoform of Musashi2. *Sci. Rep.* **7**, 1–17 (2017).

22. Pearring, J. N., Salinas, R. Y., Baker, S. A. & Arshavsky, V. Y. Protein sorting, targeting and trafficking in photoreceptor cells. *Prog. Retin. Eye Res.* **36**, 24–51 (2013).

23. Riazuddin, S. A. *et al.* A Splice-Site Mutation in a Retina-Specific Exon of BBS8 Causes Nonsyndromic Retinitis Pigmentosa. *Am. J. Hum. Genet.* **86**, 805–812 (2010).

24. Murphy, D., Singh, R., Kolandaivelu, S., Ramamurthy, V. & Stoilov, P. Alternative Splicing Shapes the Phenotype of a Mutation in BBS8 To Cause Nonsyndromic Retinitis Pigmentosa. *Mol. Cell. Biol.* **35**, 1860–1870 (2015).

25. Rachel, R. A., Li, T. & Swaroop, A. Photoreceptor sensory cilia and ciliopathies: focus on CEP290, RPGR and their interacting proteins. *Cilia* **1**, 22 (2012).

26. Veleri, S. *et al.* Ciliopathy-associated gene Cc2d2a promotes assembly of subdistal appendages on the mother centriole during cilia biogenesis. *Nat. Commun.* **5**, 1–12 (2014).

27. Zacchigna, S. *et al.* Loss of the Cholesterol-Binding Protein Prominin-1/CD133 Causes Disk Dysmorphogenesis and Photoreceptor Degeneration. *J. Neurosci.* **29**, 2297–2308 (2009).

28. Ba-Abbad, R. *et al.* Mutations in CACNA2D4 Cause Distinctive Retinal Dysfunction in Humans. *Ophthalmology* **123**, 668-671.e2 (2016).

29. Johnson, J. *et al.* Vesicular Glutamate Transporter 1 Is Required for Photoreceptor Synaptic Signaling But Not For Intrinsic Visual Functions. *J. Neurosci.* **27**, 7245–7255 (2007).

30. A simple polymerase chain reaction assay for genotyping the retinal degeneration mutation (Pdebrd1) in FVB/N-derived transgenic mice. *Lab. Anim.* **35**, 153–156 (2001).

31. Pak, J. S., Lee, E.-J. & Craft, C. M. The retinal phenotype of Grk1−/− is compromised by a Crb1rd8 mutation. *Mol. Vis.* **21**, 1281–1294 (2015).

525 32. Yousefi, M. *et al.* Msi RNA-binding proteins control reserve intestinal stem cell
526 quiescenceControl of intestinal stem cell quiescence by Msi. *J. Cell Biol.* **215**, 401–413 (2016).
527 33. Hirrlinger, P. G., Scheller, A., Braun, C., Hirrlinger, J. & Kirchhoff, F. Temporal control of gene
528 recombination in astrocytes by transgenic expression of the tamoxifen-inducible DNA recombinase
529 variant CreERT2. *Glia* **54**, 11–20 (2006).
530 34. Wright, Z. C. *et al.* ARL3 regulates trafficking of prenylated phototransduction proteins to the
531 rod outer segment. *Hum. Mol. Genet.* **25**, 2031–2044 (2016).
532 35. Wright, Z. C. *et al.* ADP-Ribosylation Factor-Like 2 (ARL2) regulates cilia stability and
533 development of outer segments in rod photoreceptor neurons. *Sci. Rep.* **8**, 1–12 (2018).
534 36. Furuta, Y., Lagutin, O., Hogan, B. L. M. & Oliver, G. C. Retina- and ventral forebrain-specific Cre
535 recombinase activity in transgenic mice. *genesis* **26**, 130–132 (2000).
536 37. Guan, W. *et al.* Eye opening differentially modulates inhibitory synaptic transmission in the
537 developing visual cortex. *eLife* **6**, e32337 (2017).
538 38. Brightman, D. S., Razafsky, D., Potter, C., Hodzic, D. & Chen, S. Nrl-Cre transgenic mouse
539 mediates loxP recombination in developing rod photoreceptors. *Genes. N. Y. N 2000* **54**, 129–135
540 (2016).
541 39. Komitova Mila, Mattsson Bengt, Johansson Barbro B. & Eriksson Peter S. Enriched Environment
542 Increases Neural Stem/Progenitor Cell Proliferation and Neurogenesis in the Subventricular Zone of
543 Stroke-Lesioned Adult Rats. *Stroke* **36**, 1278–1282 (2005).
544 40. Dilan, T. L. *et al.* ARL13B, a Joubert Syndrome-Associated Protein, Is Critical for Retinogenesis
545 and Elaboration of Mouse Photoreceptor Outer Segments. *J. Neurosci.* **39**, 1347–1364 (2019).
546 41. Perou, C. M. *et al.* Distinctive gene expression patterns in human mammary epithelial cells and
547 breast cancers. *Proc. Natl. Acad. Sci.* **96**, 9212–9217 (1999).

548 42. Abu-Qare, A. W. & Abou-Donia, M. B. Biomarkers of apoptosis: release of cytochrome c,
549 activation of caspase-3, induction of 8-hydroxy-2'-deoxyguanosine, increased 3-nitrotyrosine, and
550 alteration of p53 gene. *J. Toxicol. Environ. Health B Crit. Rev.* **4**, 313–332 (2001).
551 43. Arikawa, K. & Williams, D. S. Acetylated alpha-tubulin in the connecting cilium of developing rat
552 photoreceptors. *Invest. Ophthalmol. Vis. Sci.* **34**, 2145–2149 (1993).
553 44. Grau, M. B. *et al.* Alterations in the balance of tubulin glycylation and glutamylation in
554 photoreceptors leads to retinal degeneration. *J. Cell Sci.* **130**, 938–949 (2017).
555 45. Omori, Y. *et al.* Negative regulation of ciliary length by ciliary male germ cell-associated kinase
556 (Mak) is required for retinal photoreceptor survival. *Proc. Natl. Acad. Sci.* **107**, 22671–22676 (2010).
557 46. Susaki, K. *et al.* Musashi-1, an RNA-binding protein, is indispensable for survival of
558 photoreceptors. *Exp. Eye Res.* **88**, 347–355 (2009).
559 47. Okano, H. *et al.* Function of RNA-binding protein Musashi-1 in stem cells. *Exp. Cell Res.* **306**,
560 349–356 (2005).
561 48. Wuebben, E. L., Mallanna, S. K., Cox, J. L. & Rizzino, A. Musashi2 Is Required for the Self-Renewal
562 and Pluripotency of Embryonic Stem Cells. *PLOS ONE* **7**, e34827 (2012).
563 49. de Andrés-Aguayo, L. *et al.* Musashi 2 is a regulator of the HSC compartment identified by a
564 retroviral insertion screen and knockout mice. *Blood* **118**, 554–564 (2011).
565 50. Siddall, N. A., McLaughlin, E. A., Marriner, N. L. & Hime, G. R. The RNA-binding protein Musashi
566 is required intrinsically to maintain stem cell identity. *Proc. Natl. Acad. Sci.* **103**, 8402–8407 (2006).
567 51. Ohyama, T. *et al.* Structure of Musashi1 in a complex with target RNA: the role of aromatic
568 stacking interactions. *Nucleic Acids Res.* **40**, 3218–3231 (2012).
569 52. Sutherland, J. M., Siddall, N. A., Hime, G. R. & McLaughlin, E. A. RNA binding proteins in
570 spermatogenesis: an in depth focus on the Musashi family. *Asian J. Androl.* **17**, 529–536 (2015).

53. Uren, P. J. *et al.* RNA-Binding Protein Musashi1 Is a Central Regulator of Adhesion Pathways in Glioblastoma. *Mol. Cell. Biol.* **35**, 2965–2978 (2015).

54. Bennett, C. G. *et al.* Genome-wide analysis of Musashi-2 targets reveals novel functions in governing epithelial cell migration. *Nucleic Acids Res.* **44**, 3788–3800 (2016).

55. Rentas, S. *et al.* Musashi-2 attenuates AHR signalling to expand human haematopoietic stem cells. *Nature* **532**, 508–511 (2016).

56. Lan, L. *et al.* Human oncoprotein Musashi-2 N-terminal RNA recognition motif backbone assignment and identification of RNA-binding pocket. *Oncotarget* **8**, 106587–106597 (2017).

582 **FIGURE 1**

583

584

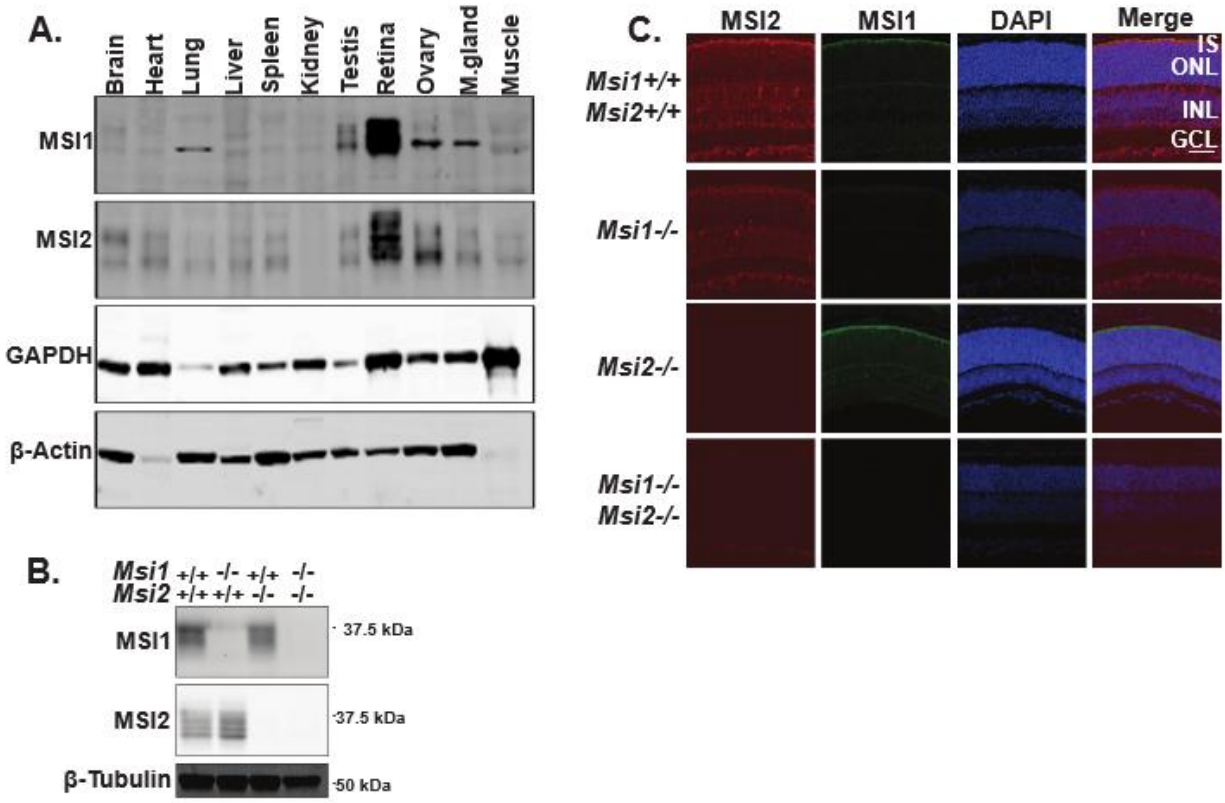

585

586

587

588 **FIGURE 2**

589

590

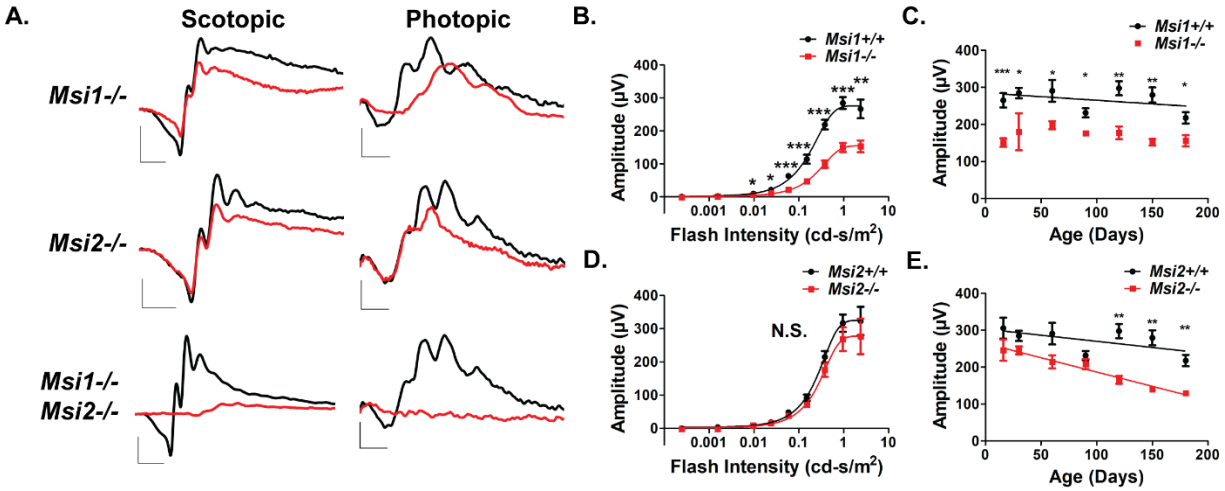

591

592

593

FIGURE 3

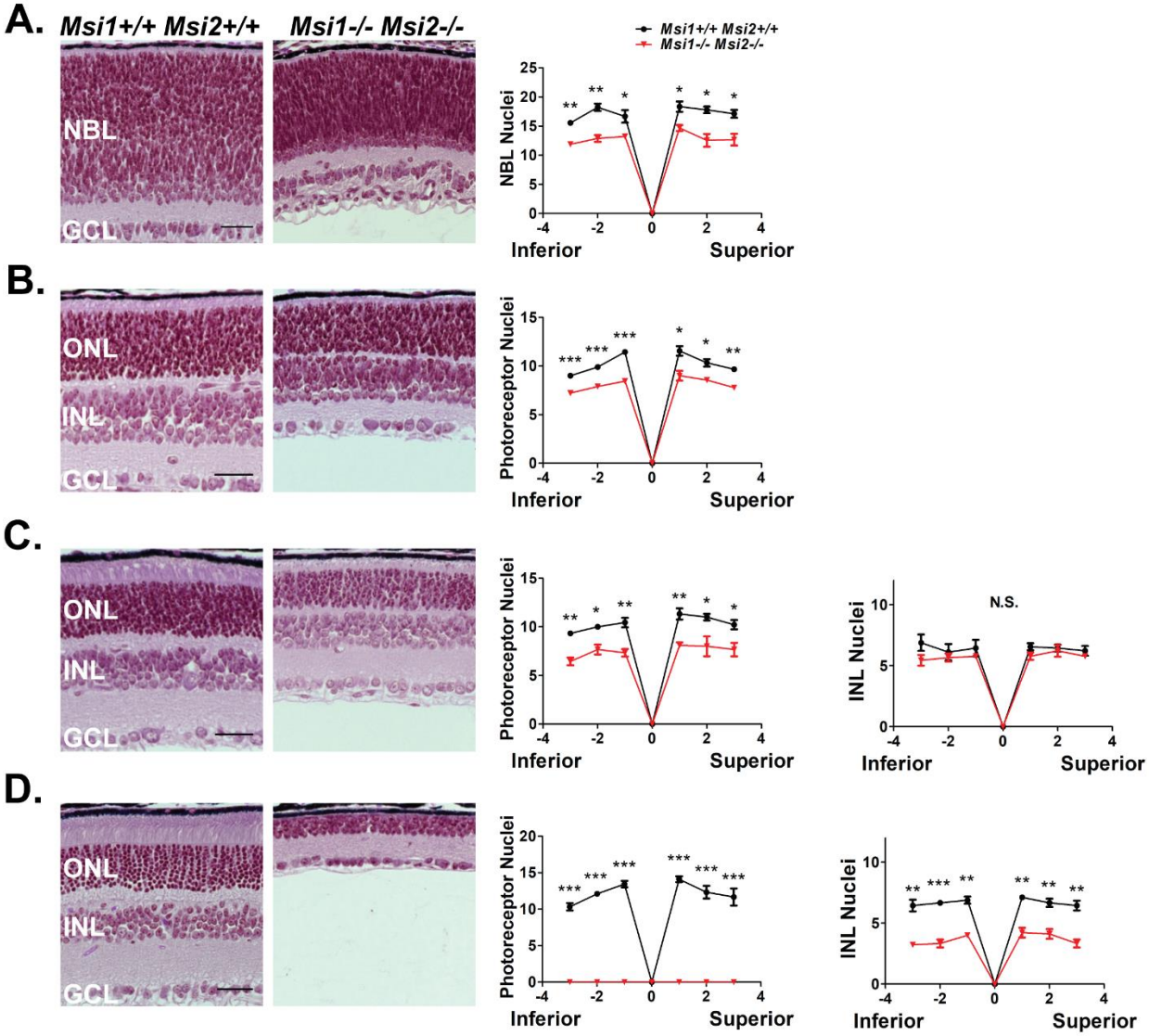

600 **FIGURE 4**

601

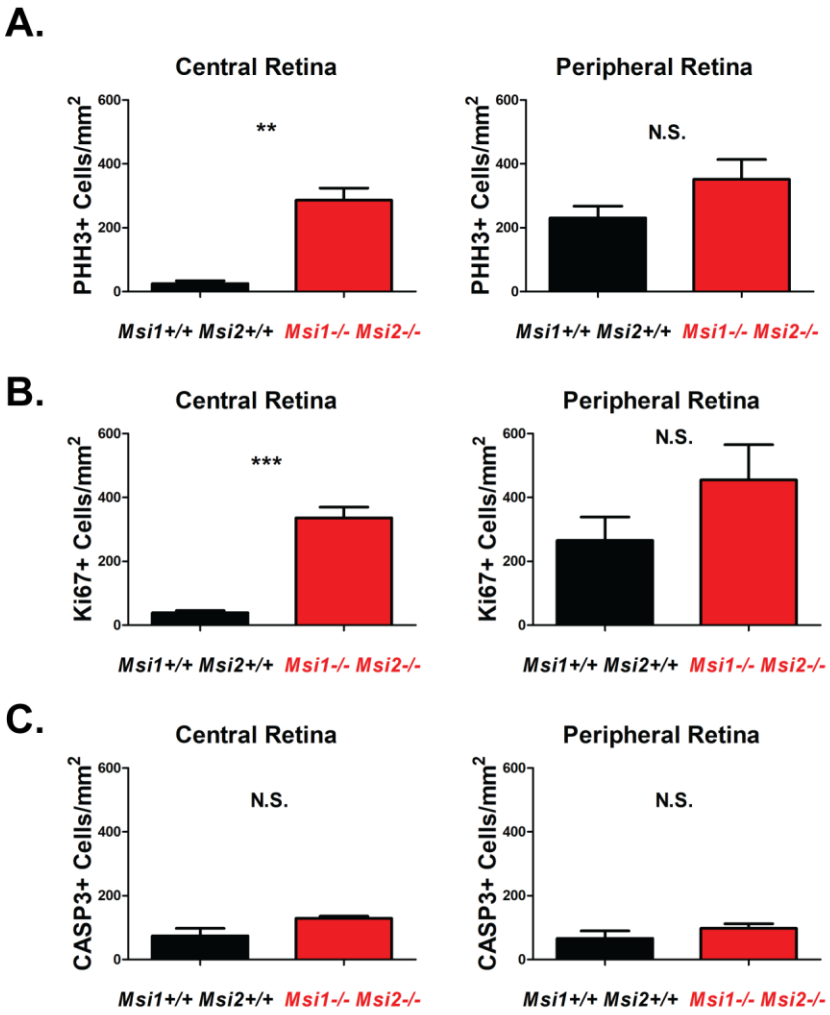

602

603

604

605 **FIGURE 5**

606

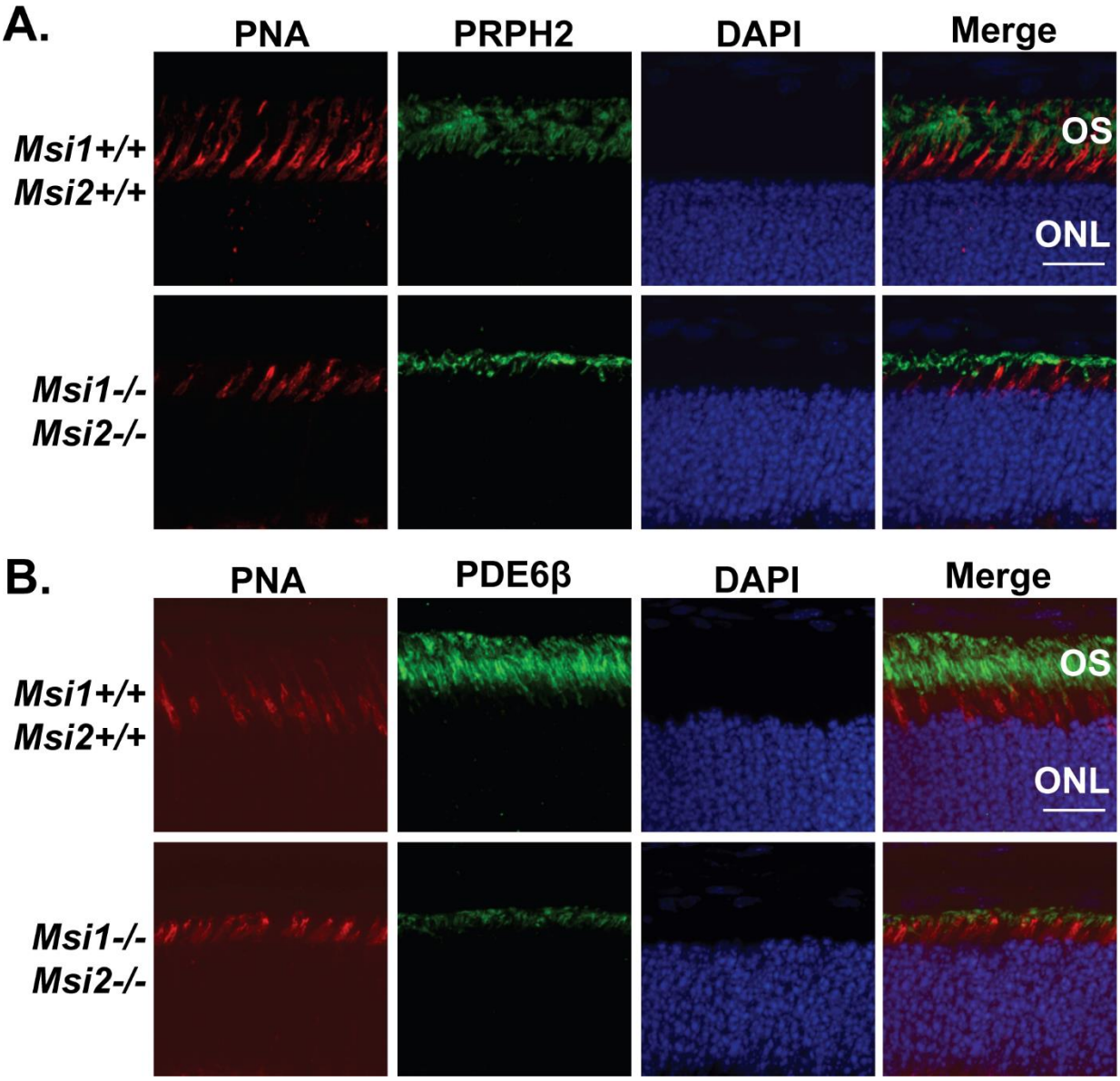

607

608

609

610 **FIGURE 6**

611

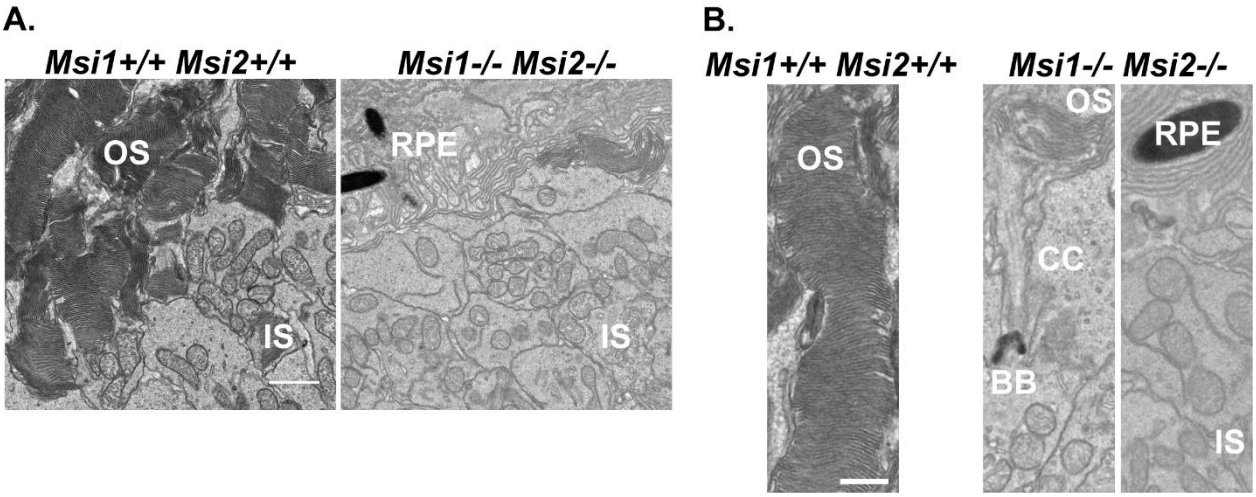

612

613

614

615 **FIGURE 7**

616

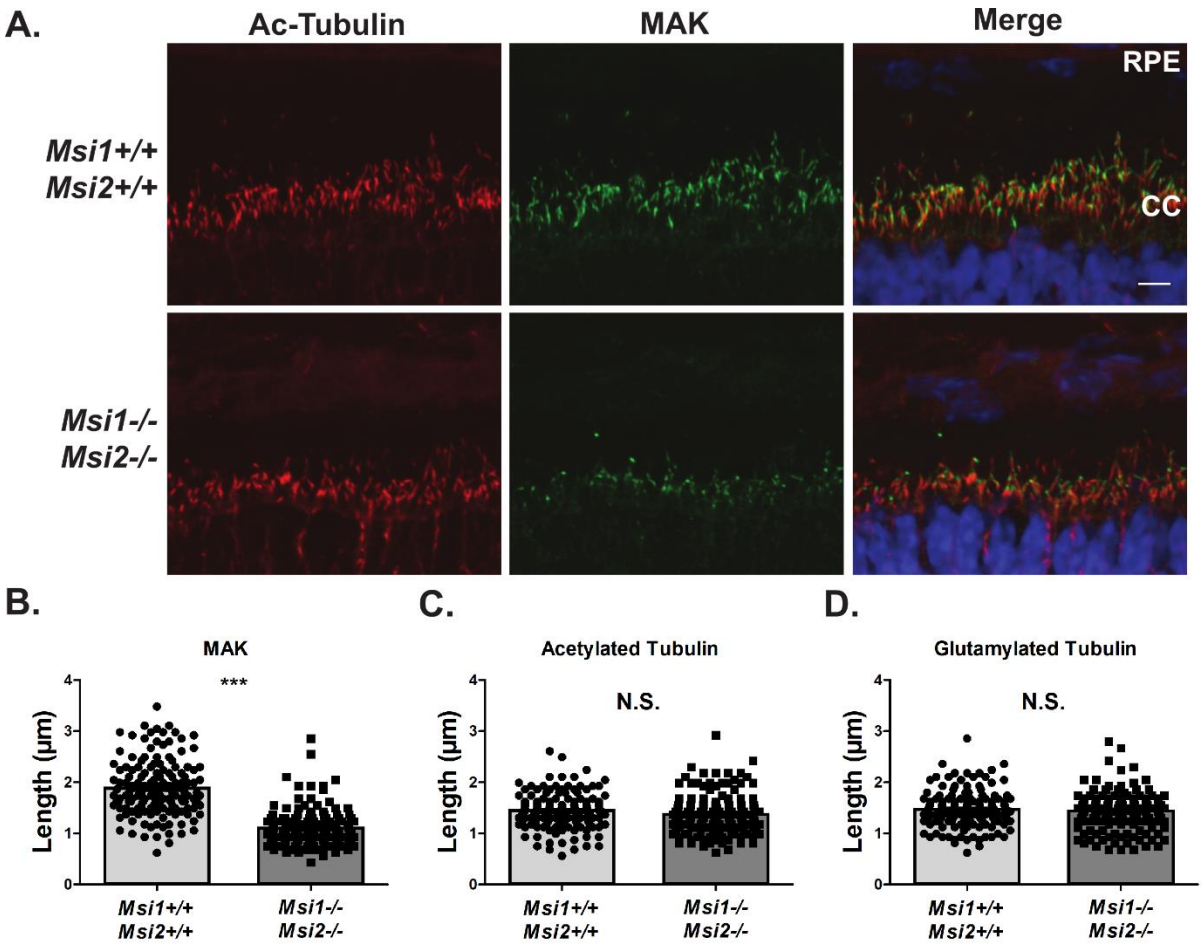

617

618

619

620 **FIGURE 8**

621

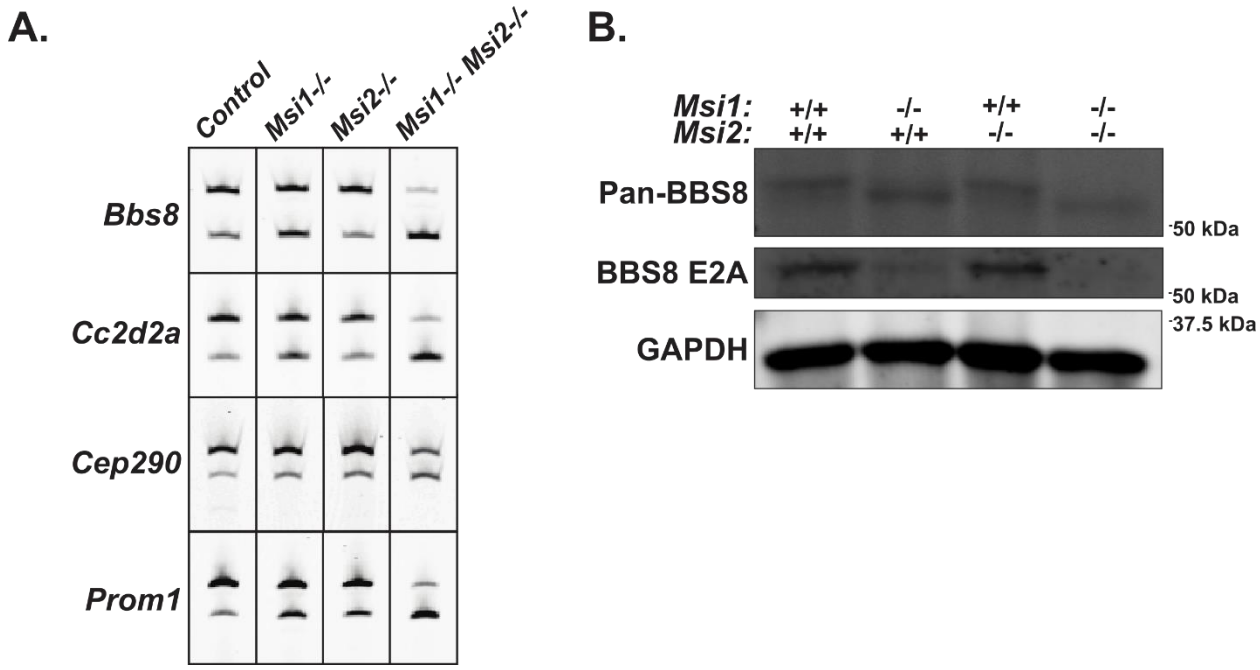

622

623

624

625 **FIGURE 9**

626

627

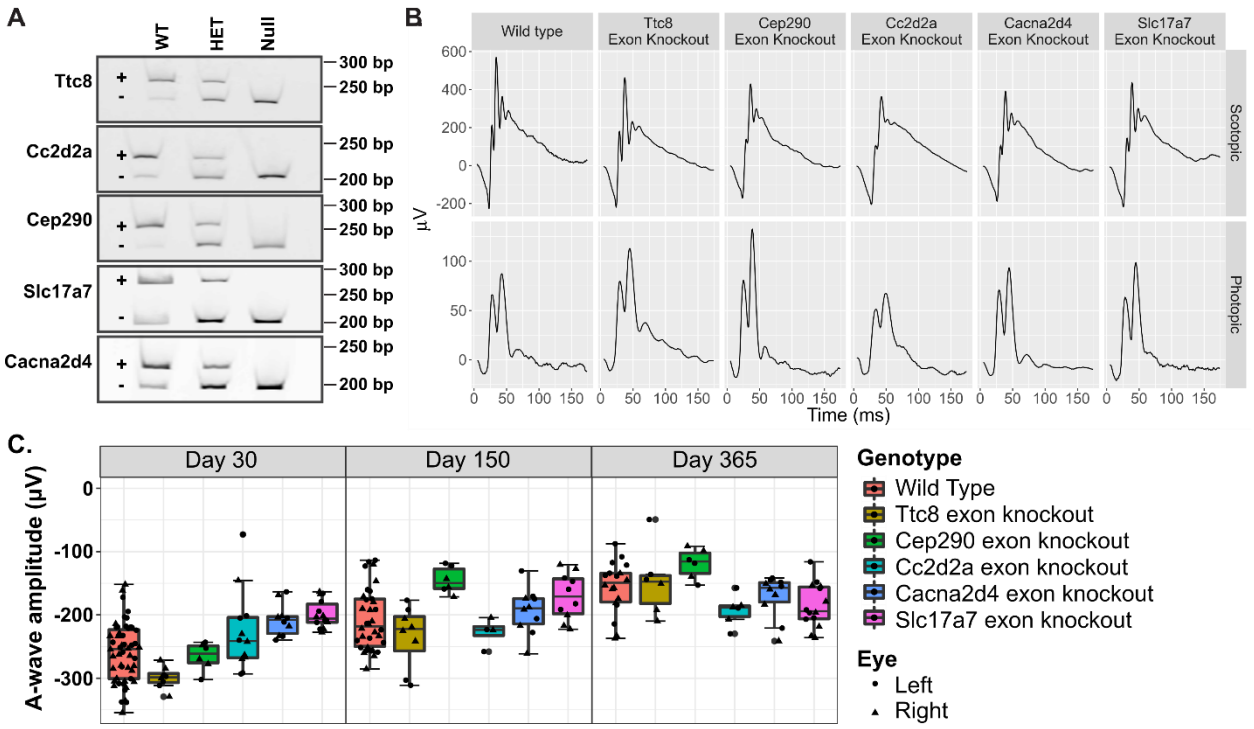

628

629

FIGURE LEGENDS

Figure 1: Conditional Musashi knockout mouse models.

A. Immunoblot of indicated tissues from adult wildtype mice probed with MSI1 and MSI2 antibodies. GAPDH and β-Actin serve as a loading control.

B. Western blot analyses of Musashi in retinal lysates from *ret-Msi1-/-*, *ret-Msi2-/-*, and *ret-Msi1-/-: Msi2-/-* mice at PN10. β-tubulin levels provide a loading control.

C. Retinal sections from *ret-Msi1-/-*, *ret-Msi2-/-*, and *ret-Msi1-/-: Msi2-/-* mice at PN10 probed with MSI1 (Green) and MSI2 (Red) antibodies along with a DAPI nuclear counterstain (Blue). (IS: inner segment, ONL: outer nuclear layer, INL: inner nuclear layer, and GCL: ganglion cell layer). Scale bar = 50μm.

Figure 2: The Musashi proteins are crucial for normal visual response.

A. Representative scotopic and photopic electroretinograms (ERGs) from the *ret-Msi1-/-*, *ret-Msi2-/-*, and *ret-Msi1-/-: Msi2-/-* mice at PN16. Scotopic ERGs were obtained after overnight dark adaptation using 0.151 cd-s/m^2 flashes while photopic ERGs were obtained with 7.6 cd-s/m^2 flashes under light-adapted conditions using a rod-saturating white background light (Scotopic scale bar: x-axis = 20ms, y-axis = 200μV; Photopic scale bar: x-axis = 20ms, y-axis = 20μV).

B. Intensity-response plot of the scotopic "a"-wave response from *ret-Msi1-/-* mice (*=P-value < 0.05; **=P-value < 0.01; ***=P-value < 0.001).

C. Plot of the rod photoreceptor "a"-wave response from *ret-Msi1-/-* mice against the age of the mouse during which the ERG was recorded.

D. Intensity-repsonse curve of the scotopic "a"-wave response from *ret-Msi2-/-* mice (*=P-value < 0.05; **=P-value < 0.01; ***=P-value < 0.001).

E. Plot of the rod photoreceptor "a"-wave response from *ret-Msi2-/-* mice plotted against the age of the mouse during which the ERG was recorded. All data is shown as the mean ± the SEM, and statistical analyses were carried out using the homoscedastic unpaired student's t-test (*=P<0.05).

Figure 3: Retinal cell death occurs in the absence of the Musashi proteins

Left: Brightfield microscopic images of H&E stained retinal cross sections from the *ret-Msi1-/-: Msi2-/-* mice at PN5 **(A),** PN10 (**B)**, PN16 **(C)**, and PN180 **(D)**.

Right: Spider plot of the layer thickness at six regions from the inferior to superior retina in the *ret-Msi1-/-: Msi2-/-* mice at PN5 (NBL: neuroblast layer, ONL: outer nuclear layer, INL: inner nuclear layer, and GCL: ganglion cell layer)

All data is shown as the mean ± the SEM, and statistical analyses were carried out using the homoscedastic unpaired student's t-test (*=P-value < 0.05; **=P-value < 0.01; ***=P-value < 0.001).

Figure 4: Increased proliferation of progenitors in the absence of MSI1 and MSI2

Quantitation of PHH3+ cells **(A)**, Ki67+ cells **(B)** and CASP3+ cells **(C)** in the central (left) and peripheral (right) regions of the retina in PN5 *ret-Msi1-/-: Msi2-/-* mice and littermate control mice.

Figure 5: The Musashi proteins are required for proper OS development

A. Immunofluorescence microscopy images of retinal cross sections from the *ret-Msi1-/-: Msi2-*

/- mice at PN16 stained with anti-peripherin-2 antibody (PRPH2: OS marker - Green) and peanut agglutinin (PNA: cone OS marker - Red) along with a DAPI nuclear counterstain (Blue).

B. Immunofluorescence microscopy images of retinal cross sections from the *ret-Msi1-/-: Msi2-/-* mice at PN16 stained with anti-phosphodiesterase-6β antibody (PDE6β: rod OS marker - Green) and peanut agglutinin (PNA: cone OS marker - Red) along with a DAPI counterstain (Blue). (OS: outer segment and ONL: outer nuclear layer). Scale bar = 20μm.

Figure 6: Abnormal development of OS in the absence of MSI1 and MSI2

A. Low magnification transmission electron microscopy images of ultrathin retinal sections from *ret-Msi1-/-: Msi2-/-* mice at PN10 visualizing the boundary between the OS and IS showing the lack of typical outer segments in the absence of the Musashi proteins (OS: outer segment, IS: inner segment, and RPE: retinal pigment epithelium). Scale bar = 2μm.

B. High magnification transmission electron microscopy images of ultrathin retinal sections from *ret-Msi1-/-: Msi2-/-* mice at PN10 visualizing the boundary between the OS and IS showing that the OS either does not form (far right) or is dysmorphic (middle) in the absence of the Musashi proteins (OS: outer segment, CC: connecting cilium, BB: basal body, RPE: retinal pigment epithelium, and IS: inner segment). Scale bar = 1μm.

Figure 7: The Musashi proteins are crucial for photoreceptor axoneme development

A. Immunofluorescence microscopy images of retinal cross sections from the *ret-Msi1-/-: Msi2-/-* mice at PN10 stained with acetylated-α-tubulin antibody (Ac-Tubulin: Red) and male germ cell-associated kinase antibody (MAK: Green) along with DAPI counterstain (Blue) (RPE: retinal pigment epithelium, CC: connecting cilium, and ONL: outer nuclear layer).

699 Scatter bar plot showing the distribution of length measurements for the photoreceptor axoneme
700 by MAK staining **(B)** and connecting cilium by Ac-tubulin staining **(C)** and glutamylated tubulin
701 staining **(D)**. Retinal sections were obtained from PN10 musashi knockouts and littermate
702 controls.
703
704 **Figure 8: The Musashi proteins regulate alternative splicing of their target transcripts**
705 **A.** Reverse transcriptase PCR splicing assay using total RNA purified from retinal lysates of *ret-*
706 *Msi1-/-*, *ret-Msi2-/-*, and *ret-Msi1-/-: Msi2-/-* mice. Ttc8, Cc2d2a, Cep290, and Prom1 are four
707 cilia- and OS-related transcripts shown to have reduced photoreceptor-specific exon inclusion in
708 the absence of MSI1 and MSI2.
709 **B.** Immunoblot of retinal lysates from *ret-Msi1-/-*, *ret-Msi2-/-*, and *ret-Msi1-/-: Msi2-/-* mice.
710 After probing with the pan-Ttc8 antibody (top), a change in the migration of the Ttc8 protein is
711 observed in the absence of MSI1 and MSI2 suggesting that the peptide encoded by Exon 2A was
712 not included. When probing with the Ttc8 E2A antibody (middle), photoreceptor-specific
713 isoform of Ttc8 was not observed in the absence of MSI1 and MSI2.
714 **Figure 9: Exon knockout mice have normal photoreceptor function**
715 **A.** Analysis of alternative splicing of the *Ttc8*, *Cc2d2a*, *Cep290*, *Slc17a7*, and *Cacna2d4* genes
716 in wild type (WT), heterozygous (Het) and homozygous (Null) exon knockouts by RT-PCR.
717 Isoforms including and skipping the alternative exon are indicated by "+" and "-", respectively.
718 **B.** Representative scotopic and photopic electroretinograms (ERGs) from wildtype, *Ttc8* exon
719 knockout, *Cep290* exon knockout, *Cc2d2a* exon knockout, *Cacna2d4* exon knockout, and
720 *Slc17a7* exon knockout mouse models at postnatal day 150. Scotopic ERGs were obtained after
721 dark adaptation while photopic ERGs were obtained under light-adapted conditions using a rod-

722 saturating white background light. No changes in photoreceptor function are observed compared
723 to control.
724 **C.** Box blot of a-wave intensities normalized to the median of the wild type a-wave at postnatal
725 days 30, 150 and 356. No significant changes in photoreceptor function of the knockouts of
726 photoreceptor specific exons in the *Ttc8*, *Cep290*, *Cc2d2a*, *Cacna2d4* and *Slc17a7* genes are
727 observed compared to the wild type control.
728
729